

# Photoresonance and conductivity of surface electrons on liquid $^3\text{He}$

Denis Konstantinov<sup>1</sup>, Yuriy Monarkha<sup>1,2</sup>, and Kimitoshi Kono<sup>1</sup>

<sup>1</sup>*Low Temperature Physics Laboratory, RIKEN, Hirosawa 2-1, Wako 351-0198, Japan*

<sup>2</sup>*B. Verkin Institute for Low Temperature Physics and Engineering of the National Academy of Sciences of Ukraine  
47 Lenin Ave., Kharkov 61103, Ukraine*

E-mail: konstantinov@riken.jp

Received October 26, 2007

Resonance variations of the in-plane conductivity of surface electrons (SEs) over liquid  $^3\text{He}$  induced by microwave (MW) radiation of a fixed frequency are experimentally and theoretically studied for low temperature scattering regimes ( $T < 0.5$  K). The system was tuned to resonance by varying the amplitude of the vertical electric field which shifts the positions of SE Rydberg levels. The line-shape change and reversing of the sign of the effect are found to be opposite to that reported previously for weak vertical electric fields. A theoretical analysis of conductivity of the SE system heated due to decay of electrons excited to the second Rydberg level by the MW explains well the line-shape variations observed. It shows also that shifting the MW resonance into the range of weak vertical fields leads to important qualitative changes in the line-shape of SE conductivity which are in agreement with observations reported previously.

PACS: **67.90.+z** Other topics in quantum fluids and solids; liquid and solid helium;  
**73.20.-r** Electron states at surfaces and interfaces;  
**73.25.+i** Surface conductivity and carrier phenomena;  
**78.70.Gq** Microwave and radio-frequency interactions.

Keywords: liquid helium, surface electrons, microwave, resonance, conductivity.

## Introduction

Surface electron (SE) states on liquid helium [1,2] are formed owing to the interplay between an attractive image potential acting above the surface,  $V_{\text{img}}(z) = -\Lambda/z$ , and a very high repulsion barrier  $V_0 \sim 1$  eV appearing at the interface ( $z = 0$ ). The image potential is very weak because  $\Lambda = e^2(\epsilon - 1)/4(\epsilon + 1)$  and the dielectric constant of liquid helium  $\epsilon$  is uniquely close to 1 ( $\epsilon - 1 \simeq 0.057$  for liquid  $^4\text{He}$ , and  $\epsilon - 1 \simeq 0.043$  for liquid  $^3\text{He}$ ). In an approximation  $V_0 \rightarrow \infty$ , SE energy levels are spaced similarly to Rydberg levels of a Hydrogen atom:  $\Delta_l = -\Delta_R/l^2$ , where  $l = 1, 2, \dots$ , and  $\Delta_R$  is the corresponding Rydberg energy which are about 7.6 K for liquid  $^4\text{He}$  and about 4.2 K for liquid  $^3\text{He}$ . The effective Bohr radius of SE Rydberg states  $a_B = \hbar^2/m_e\Lambda$  is about two orders of magnitude larger than the conventional Bohr radius, which makes these states insensitive to small surface distortions. Therefore, at low temperatures, liquid helium provides a remarkable opportunity to study a very clean two-dimensional system of highly correlated electrons. The SE

Rydberg states and a Stark effect in the vertical electric field  $E_{\perp}$  were first observed by Grimes and Brown [3] in a microwave (MW) resonance absorption experiment.

If Coulomb interaction is disregarded, SE motion along the interface can be described by the free electron spectrum  $\epsilon_k = \hbar^2 k^2 / 2m_e$ , where  $\mathbf{k}$  is a two-dimensional wave-vector. At typical helium temperatures, electron interactions with vapor atoms and capillary wave quanta (rippions) are weak enough to be treated in terms of electron scattering which limits SEs conductivity along the interface. For liquid  $^4\text{He}$  ( $^3\text{He}$ ), scattering by vapor atoms dominates at  $T > 1$  K (0.5 K), while at lower temperatures  $T < 0.5$  K (0.3 K) SEs are mostly scattered by ripples whose wave vectors  $q \leq 2k$  are much smaller than typical wave-vectors of thermal ripples. The ripplon-limited conductivity was observed by measuring the power absorption in a parallel AC electric field [4], the plasmon resonance [5] and cyclotron resonance (CR) [6] broadening.

Combined photoresonance and mobility measurements [7] were performed as an interesting indirect probe of SE Rydberg states. These measurements had shown that in the case of liquid  $^3\text{He}$  at  $T = 0.35\text{ K}$ , electron mobility decreases at the MW resonance for low powers, but the effect changes the sign for higher powers. The reduction in electron conductivity was attributed to electron-vapor atom scattering, even though this explanation was in contradiction with results of similar quantum CR measurements [6] which display an increase in SE conductivity. Of course, the comparison with quantum CR data could be misleading because in the presence of a strong magnetic field SE conductivity is affected by the many-electron effect which can lead to a substantial narrowing of the CR [8,9].

Recent conductivity measurements for SEs exposed to resonant MW radiation above liquid  $^3\text{He}$  in the vapor atom scattering regime [10] indicate that heating of the electron system is the key occurrence of a MW resonance experiment with SEs. This heating occurs because of electron decay from the excited Rydberg level to the ground level induced by interaction with vapor atoms. Because the mass of a helium atom  $M$  is much larger than the free electron mass  $m_e$ , the energy difference between the two levels is not given out but is transferred to the kinetic energy of electron motion along the interface. Under the resonance condition the effective electron temperature  $T_e$  can be much higher than the ambient temperature  $T$ . Such decay heating of SEs appears already at very low excitation rates affecting electron conductivity [10] and the MW resonance linewidth [11]. The important point is that in the vapor atom scattering regime, SE conductivity at the MW resonance steadily decreases with power, and there is no the sign change of this effect at high excitation powers similar to that reported previously [7]. At high powers, there is only saturation of the conductivity decrease caused by the quantum saturation of the fractional occupancy of the first excited level  $n_2$  approaching that of the ground level  $n_1$ . Therefore new studies of SE conductivity affected by photoresonance are necessary for understanding these interesting phenomena. An additional interest in such studies is evoked by a possible use of electrons occupying the two lowest SE Rydberg levels as electronic qubits controlled by MW radiation (for a recent review of this problem, see Ref. 12).

In this work we report the results of experimental and theoretical investigations of SE conductivity changes induced by MW resonance excitation for liquid  $^3\text{He}$  in a low temperature range ( $T < 0.5\text{ K}$ ) covering both vapor atom and ripplon scattering regimes. At  $T = 0.35\text{ K}$  and low MW powers, we observed an increase in mobility of SEs which is opposite to the result reported previously [7]. This discrepancy is explained by our theoretical analysis, which indicates that experimental results obtained at

$T \sim 0.35\text{ K}$  can be understood only if electron–ripplon interaction is taken into account. We found that the sign of the conductivity change induced by the photoresonance crucially depends on the range of the vertical (holding) electric fields  $E_{\perp}$  used for tuning of the resonant frequency. For weak holding fields,  $E_{\perp} \sim 3\text{ V/cm}$ , corresponding to the conditions of Ref. 7, conductivity indeed decreases at the MW resonance, if the excitation power is low. For holding fields used in our measurements,  $E_{\perp} \sim 93\text{ V/cm}$ , in the same power range, decay heating leads to the opposite effect — SE conductivity limited by riplons increases at the photoresonance. Because the conductivity changes induced by MW radiation occur under conditions of the linear transport regime, such hot electrons could be used for probing the electron coupling with surface excitations of Fermi-liquid  $^3\text{He}$ .

## 2. Experiment

Since DC current measurements are practically impossible for SEs on liquid helium, the capacitive detection method is frequently used for measuring conductivity [13,14]. In magnetoconductivity studies, this method employs an electrode array in the form of a Corbino disk usually placed below the helium surface. In our case, the Corbino electrodes were placed above the surface, as indicated in Fig. 1. A positive voltage  $V_B$  was applied to the bottom electrode to hold electrons. The parallel metal electrodes were separated by  $2.6 \pm 0.1\text{ mm}$ . To confine electrons laterally, each electrode was surrounded by a guard ring charged negatively (not shown in Fig. 1). To improve the heat contact between liquid  $^3\text{He}$  and the cell body, the bottom part of the cell contained a sintered silver heat exchanger. The cell was placed inside of the superconducting magnet to create magnetic field  $B$  directed perpendicular to the helium surface. One electrode of the Corbino array was driven with an AC voltage in-

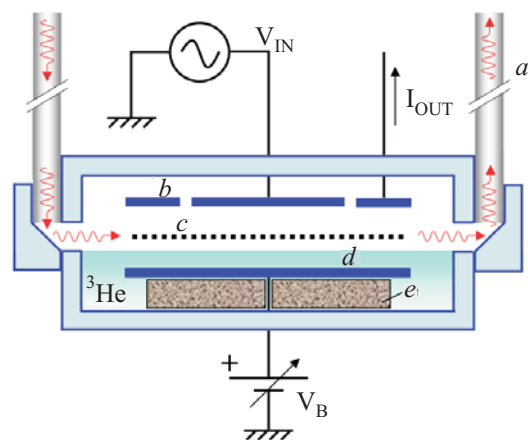


Fig. 1. Schematic drawing of the experimental setup: microwave waveguides (a), Corbino electrodes (b), surface electrons (c), bottom electrode (d), heat exchanger (e).

ducing a current in the electron layer. The measured current was analyzed by means of the transmission line model, which allows to extract  $\sigma_{xx}$  data using a conventional relationship [15].

In the cell, electrons were accumulated on the vapor-liquid  $^3\text{He}$  interface placed in the middle between the parallel metal electrodes. At typical helium temperatures, practically all electrons occupy the ground surface level ( $l=1$ ). In our measurements the areal electron density  $n_s = 1.7 \cdot 10^7 \text{ cm}^{-2}$ . To excite electrons to the second surface level ( $l=2$ ), MW radiation of a fixed frequency ( $\omega/2\pi = 130 \text{ GHz}$ ) was arranged to be passing through the cell, as shown in Fig. 1. Owing to the Stark effect, the SE system was tuned in resonance with MW radiation by varying the holding electric field  $E_{\perp}$ . A constant magnetic field was applied, and the Corbino signal was recorded as  $E_{\perp}$  was swept through the resonance. In order to avoid complications with many electron effects affecting quantum magnetotransport of SEs on liquid helium, we employed only a weak magnetic field for which the magnetoconductivity can be described by the classical Drude equation

$$\sigma_{xx} = \frac{e^2 n_s}{m_e} \frac{\nu}{\nu^2 + \omega_c^2}, \quad (1)$$

where  $\omega_c$  is the cyclotron frequency, and  $\nu$  is the collision frequency describing momentum relaxation of SEs. For example, at  $T = 0.35 \text{ K}$ , the magnetic field  $B$  was about  $233 \text{ G}$  which is within the semi-classical transport regime ( $\hbar\omega_c \ll T$ ). Of course, the frequency  $\omega$  of the AC voltage  $V_{IN}$  is too much lower than  $\omega_c$  and  $\nu$  to be taken into account in the Drude equation. Extracting  $\nu$  from the magnetoconductivity data we can judge of the DC conductivity of SEs in the absence of the magnetic field  $\sigma = e^2 n_s / m_e \nu$  and compare its variations induced by MW with the old results of Ref. 7.

The MW resonance itself can be described by the usual Lorentzian form determining the stimulated absorption (emission) rate [16]

$$r_{12} = \frac{0.5\Omega^2\gamma}{\gamma^2 + [\omega - \omega_{21}(E_{\perp})]^2}, \quad (2)$$

where  $\omega_{21} = (\Delta_2 - \Delta_1) / \hbar$  is the resonant frequency depending on the holding electric field,  $\gamma$  is the half-width calculated previously in Ref. 17,  $\Omega = eE_{MW} \langle 1 | z | 2 \rangle / \hbar$  is the Rabi frequency,  $E_{MW}$  is the MW field amplitude,  $\langle 1 | z | 2 \rangle$  is the electric dipole length for the transition. For low excitation, the energy absorbed from the MW field is proportional to  $\hbar\omega_{21}r_{12}$ . Since  $\gamma \ll \omega_{21}$ , the excitation rate and energy absorption as functions of  $E_{\perp}$  have a sharp resonance structure when  $\omega_{21}(E_{\perp})$  is close to the MW frequency  $\omega$ .

Variations in electron collision frequency  $\nu(E_{\perp})$  obtained from our magnetoconductivity data, as described above, are shown in Fig. 2. At  $T = 0.48 \text{ K}$ , the electron collision frequency has a typical resonance structure with a maximum positioned at  $E_{\perp} = 93 \text{ V/cm}$ . Thus, under the condition, the MW resonance excitation leads to a decrease in SE conductivity, as expected for the vapor atom scattering regime [10]. In this case, the increase in the collision rate is caused by decay heating of SEs and their occupation of higher surface levels, where the inter-level collision rate is high.

The recording signal greatly changes, if the ambient temperature  $T = 0.35 \text{ K}$  which corresponds to the conditions and results of Ref. 7 discussed in the Introduction. The most important conclusion which comes out from Fig. 2 for this case is that MW radiation leads to an increase in conductivity ( $\sigma = e^2 n_s / m\nu$ ) at low powers. This is opposite to the result of Ref. 7. The resonance line in

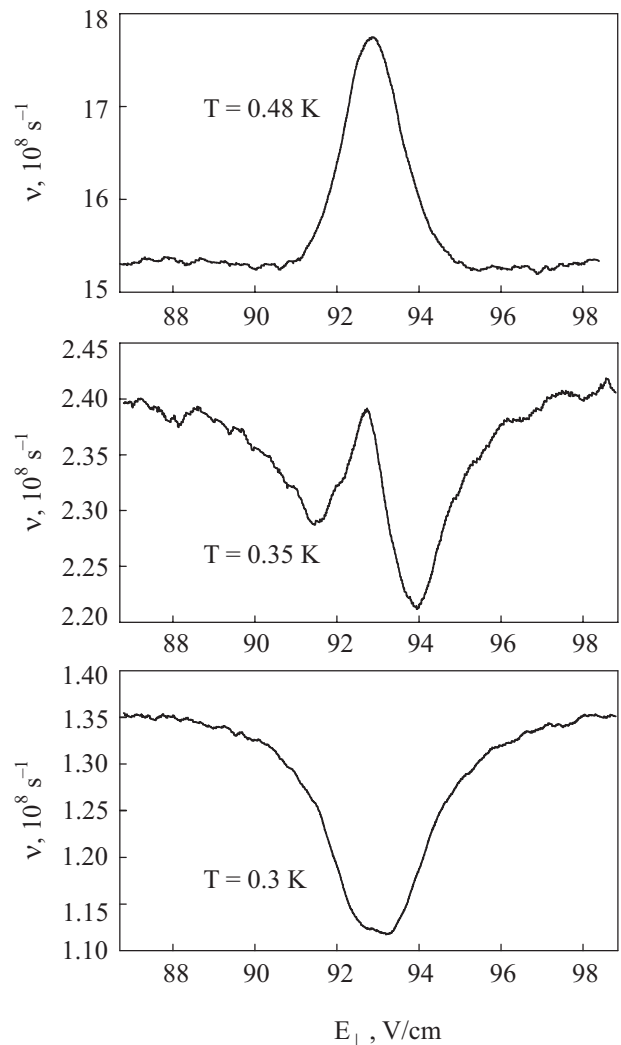


Fig. 2. Variations of the effective collision frequency with  $E_{\perp}$  induced by MW radiation and measured at three typical ambient temperatures.

not of the Lorentzian shape and the effect changes the sign as  $E_{\perp}$  approaching the resonance value. It is clear that the sign change of the effect is due to the contribution from vapor atom scattering. Therefore, the conductivity increase in the region of resonance tails is, obviously, due to electron-rippion scattering. This conclusion is confirmed also by the data obtained at  $T = 0.3$  K, when vapor atom scattering is substantially reduced. For such conditions, the dependence  $v(E_{\perp})$  has a usual resonance shape, but the sign of its variations with  $E_{\perp}$  is opposite to that obtained in the vapor atom scattering regime ( $T = 0.48$  K). Scattering by vapor atoms only slightly affects the resonance curve near its minimum. Since our new low temperature data conflict with the data reported in Ref. 7, the situation should be clarified by an appropriate theoretical analysis.

### 3. Theory

#### 3.1. Decay heating

For the vapor atom scattering regime, it is proven that even a very small fraction of SE excited by the MW from the first to the second surface level can substantially heat the entire electron system [10,18]. This happens because the decay rate of electrons occupying the second surface level  $\tau_{21}^{-1}$  is determined mostly by electron interaction with heavy vapor atoms. Therefore, a return of an electron back to the ground level is accompanied by a very small energy exchange between an electron and a vapor atom. Thus, practically all the excitation energy  $\Delta_{21}$  (here and below  $\Delta_{ll'} = \Delta_l - \Delta_{l'}$ ) is transferred to the kinetic energy of electron motion along the interface which is eventually redistributed between other electrons because of electron-electron collisions. At the same time, the energy relaxation rate  $\tilde{v}$  for electron-atom scattering is much lower than the decay rate of the first excited level  $\tau_{21}^{-1}$ . This leads to a strong increase in electron temperature even at very low excitation rates  $r_{12}\tau_{21} \sim 10^{-3}$ .

Determination of electron temperature requires the knowledge of the electron energy relaxation rate due to interaction with scatterers for arbitrary level occupancies. Decay heating leads to electron occupation of higher surface levels, therefore outer levels ( $l > 2$ ) cannot be disregarded in the expression for the energy relaxation rate [18]

$$\tilde{v}_a = \frac{m_e}{M} v_a^{(0)} \sum_{l,l'} n_l \exp[-(|\Delta_{ll'}| + \Delta_{ll'}) / 2T_e] \times \left[ \frac{\Delta_R}{T_e} u_{ll'} + \left( \frac{|\Delta_{ll'}|}{T_e} + 2 \right) s_{ll'} \right], \quad (3)$$

where  $\Delta_R = \hbar^2 / 2m_e a_B^2$ , and  $n_l = N_l / N_e$  are fractional occupancies of surface levels. We used

$$v_a^{(0)} = \frac{m_e n_a V_a^2}{\hbar^3 B_{11}},$$

$$s_{ll'} = \frac{B_{11}}{B_{ll'}}, \quad B_{ll'}^{-1} = \int_0^{\infty} dz [f_l(z) f_{l'}(z)]^2, \quad (4)$$

$$u_{ll'} = \frac{a_B^2 B_{11}}{C_{ll'}}, \quad C_{ll'}^{-1} = \int_0^{\infty} dz \left\{ \frac{d}{dz} [f_l(z) f_{l'}(z)] \right\}^2, \quad (5)$$

where  $n_a$  is the density of vapor atoms,  $f_l(z)$  are electron wavefunctions describing surface states,  $V_a$  is the amplitude of the pseudo-potential  $V_a \delta(\mathbf{R}_e - \mathbf{R}_a)$  frequently used for description of the electron-atom interaction, and  $v_a^{(0)}$  is the momentum relaxation rate of SEs for scattering within the ground surface level ( $l = l' = 1$ ). In terms of  $\tilde{v}_a$  the power transfer can be written as  $(T_e - T) \tilde{v}_a (T_e)$ .

For electron-rippion scattering, energy relaxation is much more complicated. Scattering processes which involve only one ripplon also can be considered as quasi-elastic, because the energy exchange  $\hbar\omega_q$  is very small for  $q \leq 2k$ . Energy relaxation is much more effective, when electrons emit couples of shortwave riplons with small total wave vectors ( $|\mathbf{q} + \mathbf{q}'| \ll q$ ) [19]. In this case, the energy exchange  $2\hbar\omega_q$  at a scattering event is of the order of  $T_e$  and the energy transfer rate to the environment increases by about two orders of magnitude. Because of the strong repulsion barrier existing at the interface  $V_0$ , the largest contribution to the energy relaxation rate is given from the nonlinear interaction term [2]

$$V_{\text{int}}^{(2)}(z, \mathbf{r}) = \frac{1}{2} \frac{\partial^2 V_e^{(0)}}{\partial z^2} \xi^2(\mathbf{r}), \quad (6)$$

where  $V_e^{(0)}$  is the electron potential for the flat interface, and  $\xi(\mathbf{r})$  is the surface displacement operator. The matrix elements of  $V_{\text{int}}^{(2)}$  describe two-rippion scattering probabilities already in the second order of the perturbation theory.

The matrix elements  $g_{ll'} \equiv 0.5(\partial^2 V_e^{(0)} / \partial z^2)_{ll'}$  [here  $(\dots)_{ll'}$  means  $\langle l | \dots | l' \rangle$ ] can be expressed in terms of the derivative of the electronic wave functions  $f_l'(z)$  at the helium surface ( $z = 0$ ) calculated in the approximation  $V_0 = \infty$ . This results in

$$g_{ll'} \simeq V_0 \kappa_0^{-1} f_l'(0) f_{l'}'(0) = \kappa_0 \sqrt{\left( \frac{\partial v}{\partial z} \right)_{ll'} \left( \frac{\partial v}{\partial z} \right)_{l'l}}, \quad (7)$$

where  $\kappa_0^{-1} = \hbar / \sqrt{2m_e V_0}$  is the penetration depth of the electron wavefunction into liquid, and  $v(z) = -\Lambda / z + eE_{\perp} z$ . Since  $(\partial v / \partial z)_{ll'}$  is finite in the limiting case  $V_0 \rightarrow \infty$ , the matrix elements  $g_{ll'} \propto \sqrt{V_0}$ .

Following the previously described procedure [20], the energy loss of SEs per unit time can be presented in



the conventional form  $\dot{\mathcal{E}} = -N_e \tilde{\nu}_{2r}(T_e)(T_e - T)$  with the energy relaxation rate defined as

$$\begin{aligned} \tilde{\nu}_{2r} = & \frac{m}{2\pi\rho^2(T_e - T)} \sum_{l'l} |g_{ll'}|^2 n_l \int_0^\infty dq \frac{q^3}{\omega_q} (N_q + 1)^2 \times \\ & \times \left\{ 1 - \frac{n_{l'}}{n_l} \exp \left[ \frac{\Delta_{l'l}}{T_e} - \frac{2\hbar\omega_q}{T_e T} (T_e - T) \right] \right\} \times \\ & \times \exp \left[ -\frac{|\Delta_{l'l} + 2\hbar\omega_q| + \Delta_{l'l} + 2\hbar\omega_q}{2T_e} \right], \quad (8) \end{aligned}$$

where  $N_q$  is the ripplon distribution function and  $\rho$  is the liquid helium mass density. A detailed analysis of Eq. (8) indicates that this expression is positive. For the Boltzmann distribution of level occupancies  $n_l$  and  $l=l'=1$ , this expression transforms into the result obtained in Ref. 20.

Equation (8) shows that for two-riplon emission within the surface levels ( $l=l'$ ), typical riplons contributed to  $\tilde{\nu}_{2r}$  belong to the short wavelength range  $2\hbar\omega_q \sim T_e$ . In the case of liquid  $^3\text{He}$ , the behavior of the surface excitation spectrum in this range is unknown. It is not known also how the strong damping of riplons expected at low temperatures affects the scattering probabilities. Anyway, experimental data indicate that the strong damping of capillary waves does not affect much one-riplon scattering probabilities which determine the momentum relaxation of SEs. Therefore, in our numerical evaluations of  $\tilde{\nu}_{2r}$  we shall disregard damping effects and assume that even in the short wavelength range the ripplon spectrum coincides with the capillary wave asymptote  $\omega_q = \sqrt{\alpha/\rho} q^{3/2}$ .

The electron temperature is determined by the energy balance equation

$$(n_1 - n_2)\Delta_{21}r_{12} = (T_e - T)\tilde{\nu}(T_e), \quad (9)$$

where  $\tilde{\nu}(T_e)$  is the total energy relaxation rate due to vapor atoms and riplons. At the same time, fractional occupancies  $n_l$  should be obtained from the rate equations  $dn_l/dt=0$  which ensure the balance between electron transition to and from surface levels caused by scatterers and the MW field. In the case of electron-vapor atom interaction, scattering frequencies which enter the rate equations for level occupancies have a very simple form

$$w_{l \rightarrow l'}^{(a)} = v_a^{(0)} s_{ll'} \exp[-(|\Delta_{l'l}| + \Delta_{l'l})/2T_e]. \quad (10)$$

For transitions down the surface levels ( $l > l'$  and  $\Delta_{l'l} < 0$ ), the scattering rate  $w_{l \rightarrow l'}^{(a)}$  does not depend on  $T_e$ , while for scattering up ( $l < l'$ ,  $\Delta_{l'l} > 0$ ), the scattering rate  $w_{l \rightarrow l'}^{(a)}$  acquires an additional exponential factor  $e^{-\Delta_{l'l}/T_e}$ .

If electron-riplon scattering dominates, at  $T > 0.1$  K, the scattering frequencies are determined mostly by

one-riplon processes. Collecting corresponding probabilities found in the framework of the usual perturbation treatment, the scattering rates can be presented in the following form

$$\begin{aligned} w_{l \rightarrow l'}^{(lr)} = & \frac{T}{4\sqrt{\pi}\alpha\hbar\sqrt{T_e}} \int_0^\infty \frac{d\varepsilon_q}{\varepsilon_q \sqrt{\varepsilon_q}} |\langle l' | U_q | l \rangle|^2 \times \\ & \times \exp[-(\varepsilon_q + \Delta_{l'l})^2 / (4\varepsilon_q T_e)], \quad (11) \end{aligned}$$

where  $\varepsilon_q = \hbar^2 q^2 / 2m_e$ . The matrix elements of the electron-riplon coupling  $U_q$  can be written as [2]  $\langle l' | U_q(z) | l \rangle = (eE_q)_{ll'} + F_{ll'}$ , where

$$eE_q(z) = \Lambda q^2 \left[ \frac{1}{(qz)^2} - \frac{K_1(qz)}{qz} \right], \quad (12)$$

$$F_{ll'} = eE_\perp \delta_{ll'} + \Phi_{ll'},$$

$$\Phi_{ll'} = - \left( \frac{\partial V_e^{(0)}}{\partial z} \right)_{ll'} = \frac{\hbar^2}{2m_e} f_l'(0) f_{l'}'(0) - \left( \frac{\partial v}{\partial z} \right)_{ll'}, \quad (13)$$

and  $K_1(x)$  is the modified Bessel function of the second kind. It is obvious that  $w_{l' \rightarrow l}^{(lr)} = w_{l \rightarrow l'}^{(lr)} \exp(-\Delta_{l'l}/T_e)$ . Since  $\Phi_{ll} = 0$ , diagonal matrix elements of  $U_q$  are determined only by the holding field term  $eE_\perp$  and the term  $eE_q$  which originates from the polarization interaction with oscillating liquid. For off-diagonal terms,  $\Phi_{ll'}$  substitutes the holding field term which turns to zero.

At  $T > 0.1$  K, the decay rate of excited SE states is determined mostly by quasielastic one-riplon scattering, while the energy relaxation is mostly due to inelastic two-riplon scattering discussed above. Electron scattering induced by one-riplon processes limits the lifetime of the first excited Rydberg level and transfers the energy difference  $\Delta_{21}$  into the kinetic energy of electron motion along the interface. Then electron-electron collisions which have the highest rate redistribute it among other electrons forming a nondegenerate distribution of the in-plane momentum with an effective electron temperature  $T_e > T$ . With much lower rate (about  $10^6 \text{ s}^{-1}$ ) all the electrons transfer the energy to the environment emitting couples of short wavelength riplons. Therefore, decay heating of SEs at the MW resonance is expected in the ripplon scattering regime as well. At much lower temperatures, the one-riplon contribution to the decay rate of excited surface levels freezes out and one have to take into account two-riplon emission processes [21] which start to limit the lifetime of excited surface levels. Still, this limiting case, which requires a separate examination, is beyond the conditions of the experiments discussed above.

To obtain the electron temperature at the MW resonance ( $\omega = \omega_{21}$ ) as a function of the Rabi frequency, we

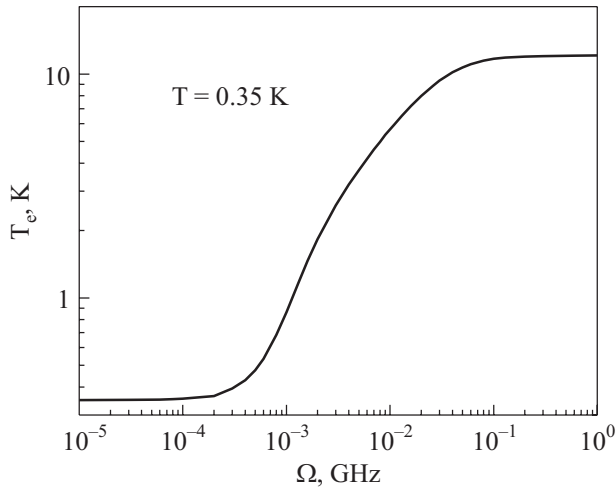


Fig. 3. Electron temperature at the MW resonance vs the Rabi frequency calculated for  $T = 0.35$  K and  $E_{\perp} = 93$  V/cm.

found numerical solutions of the energy balance equation and the rate equations for  $n_l$  under different experimental conditions. Typical dependence  $T_e(\Omega)$  at the resonance maximum is shown in Fig. 3. In these calculations, the wave functions of the first 10 levels were obtained by means of numerical solution of the corresponding Schrodinger equation, while the next 190 levels were approximately described by Airy functions. At the beginning, with an increase in the Rabi frequency,  $T_e$  increases fast. Then, at high excitations ( $r_{12}\tau_{21} > 1$ ), electron temperature saturates due to the saturation of the level occupancy of the first excited level  $n_2 \rightarrow n_1$ . Figure 3 indicates that electron temperatures of about 10 K can be reached at the saturation condition. For a fixed  $\Omega$ , electron temperature decreases with  $|\omega - \omega_{21}(E_{\perp})|$  in accordance with Eq. (2), because it reduces the excitation rate  $r_{12}$ .

### 3.2. Conductivity of hot electrons

It is clear that decay heating of SEs is a very important effect induced by the MW resonance. In the vicinity of the resonance one can have ultra-hot electrons covering the cold surface of liquid helium ( $T_e \gg T$ ). For weak driving electric fields, conductivity of such hot electrons can be described by the linear transport theory. Additionally, in this system, electron–electron collisions are usually much higher than other relaxation rates which allows us to simplify the conductivity treatment. To obtain the effective collision frequency  $\nu$  which enters the Drude conductivity equation we can just evaluate the kinetic friction acting on the whole electron system, assuming that in the moving reference frame, the electron liquid can be described by the equilibrium dynamical structure factor [2]. Gener-

ally, the kinetic friction can be represented as  $\mathbf{F}_{\text{fric}} = -N_e m_e \nu \mathbf{V}_{av}$ , where  $\mathbf{V}_{av}$  is the average velocity.

For the vapor atom scattering regime, the effective collision frequency which determines DC conductivity ( $\sigma = e^2 n_s / m_e \nu$ ) has a simple form [18]

$$\nu^{(a)} = \nu_0^{(a)} \sum_{l,l'} s_{l'l} n_l \exp\left(-\frac{|\Delta_{l'l}| + \Delta_{l'l}}{2T_e}\right) \left[1 + \frac{|\Delta_{l'l}| + \Delta_{l'l}}{2T_e}\right]. \quad (14)$$

There are two important factors which cause changes in  $\nu^{(a)}$ , if SE are heated. The first factor is the electron occupation of high surface levels which increases inter-level scattering and the momentum relaxation rate  $\nu^{(a)}$ . The second factor is a decrease in matrix elements  $s_{l'l}$  with level numbers which acts in the opposite way. It is remarkable that the outcome of the competition of these two factors strongly depends on the holding electric field. For typical holding fields used in our experiments ( $E_{\perp} \sim 100$  V/cm), the first factor dominates and the effective collision frequency  $\nu^{(a)}$  increases with  $\Omega$  without an observable sign of a decrease [10]. Nevertheless, our new calculations conducted for weak holding fields ( $E_{\perp} = 3.15$  V/cm) related to the experiment of Ref. 7 results in a more complicated behavior of  $\nu^{(a)}(\Omega)$  shown in Fig. 4. At low powers,  $\nu^{(a)}$  decreases with the MW excitation by about 4%, and then we have the sign change of the effect. This decrease is induced by the reduction in matrix elements  $s_{l'l}$  whose magnitude depends strongly on  $E_{\perp}$ . Thus, for weak holding fields scattering by vapor atoms should be reduced by MW radiation at low powers, which is opposite to the mobility decrease at the photoresonance reported previously [7]. This means that vapor atom scattering cannot be the origin of that mobility decrease.

The ripplon contribution to the momentum collision frequency of SEs can be obtained similarly to Eq. (11)

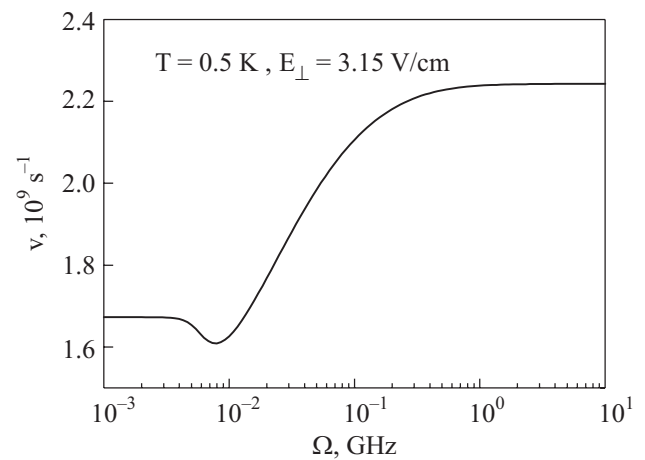


Fig. 4. Collision frequency at the MW resonance vs the Rabi frequency calculated for the vapor atom scattering regime.

$$\begin{aligned}
 v^{(r)} = & \frac{T}{4\sqrt{\pi}\alpha\hbar T_e} \sum_l n_l \int_0^\infty \frac{d\varepsilon_q}{\varepsilon_q} \sum_{l'} | \langle l' | U_q(z_e) | l \rangle |^2 \times \\
 & \times \frac{(\varepsilon_q + \Delta_{l'l})}{\sqrt{\varepsilon_q 4T_e}} \exp \left[ -\frac{(\varepsilon_q + \Delta_{l'l})^2}{4\varepsilon_q T_e} \right]. \quad (15)
 \end{aligned}$$

The additional factor of the integrand containing  $(\varepsilon_q + \Delta_{l'l})$  originates from the factor  $\mathbf{qk}$  which usually enters the equation for the momentum relaxation rate. In our evaluations of matrix elements  $\langle l' | U_q(z_e) | l \rangle$ , we shall use the variational form of SE wave functions  $f_l(z) = A_l z P_l(z) \exp[-b_l z / 2]$ , where  $A_l$  is the normalization constant,  $P_l(z)$  is a polynomial of power  $l-1$ . We shall use also the following notations  $b_{ll'} = (b_l + b_{l'}) / 2$ .

To understand the origin of strange variations in  $v^{(r)}$  induced by decay heating, it is convenient to rearrange the collision rate of electrons using the specific form of electron-rippion coupling and the Boltzmann approximation for fractional occupancies  $n_l = n_l^{(B)}$ . The latter works well for low and medium excitations and fails under the saturation condition [18]. In this approximation, using  $v^{(r)} = \sum_l n_l^{(B)} v_l^{(r)}$ , we introduce the collision frequency of electrons occupying a level  $l$ ,

$$\begin{aligned}
 v_l^{(r)} = & \frac{T}{4\alpha\hbar T_e} \sum_{l'} F_{ll'}^2 \exp \left[ -\frac{|\Delta_{l'l}| + \Delta_{l'l}}{2T_e} \right] + \\
 & + \frac{4TT_e}{\sqrt{\pi}\alpha\hbar a_B^2} \sum_{l'} \int_0^\infty x^{1/2} \exp \left[ -\frac{(x + \Delta_{l'l} / 4T_e)^2}{x} \right] \times \\
 & \times \left[ x W_{ll'}^2(x) \frac{4T_e}{\varepsilon_{b_{ll'}}} + \frac{F_{ll'} a_B}{2T_e} W_{ll'}(x) \frac{4T_e}{\varepsilon_{b_{ll'}}} \right] dx, \quad (16)
 \end{aligned}$$

where functions  $W_{ll'}(y)$  are defined by

$$\begin{aligned}
 W_{ll'}(y) = & \frac{2A_l A_{l'}}{b_{ll'}^3} \int_0^\infty \exp(-x) P_l(x / b_{ll'}) P_{l'}(x / b_{ll'}) \times \\
 & \times \left[ \frac{1}{y} - x \frac{K_1(x\sqrt{y})}{\sqrt{y}} \right] dx, \quad (17)
 \end{aligned}$$

and  $\varepsilon_{b_{ll'}}$  is defined similar to  $\varepsilon_q$  with  $b_{ll'}$  standing for  $q$ . Usually, low temperature asymptotes of  $W_{ll'}(y)$  valid for  $y \ll 1$  are used for specific evaluations, such as mobility calculations [22] and the nonlinear conductivity studies [23]. For example, in this approximation,  $W_{11}(y) \simeq \simeq 0.5 \ln(4/y) - 1$ . In our treatment of hot electrons, we cannot restrict ourselves to this approximation because  $4T_e$  can be of the order of  $\varepsilon_{b_{ll'}}$ .

In spite of the cumbersome form of Eq. (16), the main features of  $v_l^{(r)}$  can be seen quite easily. In contrast with  $v_0^{(a)}$ , the electron-rippion collision frequency for electron scattering within the ground level depends strongly

on  $T_e$ . For  $l = l' = 1$ , the first term of Eq. (16), representing the holding field term  $eE_\perp$  of  $U_q$ , decreases with electron temperature as  $T_e^{-1}$ . The second term of Eq. (16) has a more complicated dependence on  $T_e$ . Nevertheless, it is quite clear that for warm SEs the term whose integrand contains  $W_{ll'}^2$  increases with electron temperature approximately as  $T_e \ln^2(\varepsilon_{b_l} / T_e)$ , because the low temperature asymptote of  $W_{11}(y)$  given above has only logarithmic dependence on  $y$ . At higher  $T_e$ , when  $4\varepsilon_{b_l} / T_e \sim 1$ , we can simplify  $W_{11}(y) \approx 1/3\sqrt{y}$  and the second term becomes approximately independent of  $T_e$ . With further increase in  $T_e$ , when the argument of  $W_{11}$  becomes large, even this term start decreasing with electron temperature. Thus, we conclude that the integral effect of decay heating on  $v^{(r)}$  depends strongly on the magnitude of the holding electric field  $E_\perp$ . For zero or a weak value of  $E_\perp$ , the collision rate starts to increase with warming of SEs, then attains a maximum and starts to decrease. If the holding field is sufficiently strong, the collision rate decreases with heating even for warm SEs ( $T_e \gtrsim T$ ).

#### 4. Results and discussions

The momentum collision rate  $v^{(r)}$  given by Eqs. (15) and (16) has a very complicated form, which is not convenient for evaluations when many surface levels should be taken into account. In this case, there are two options: one can simplify the electron-rippion coupling, or take into account only a very restricted number of surface levels. In this work, we consider only 1 and 3-level models with the exact form of  $U_q$ . The wave functions of surface levels are found according to the conventional variational principle.

For electron-vapor atom scattering, the momentum relaxation rate given in Eq. (14) is much more simple, and, therefore, it can be evaluated for a large number of surface levels sufficient for the convergence of the result, if we approximate higher levels ( $l > 3$ ) by the corresponding Airy functions. This allows us to take into account up to 400 surface levels. The chosen approximation is expected to describe well the conductivity of hot SEs for strong holding fields ( $E_\perp \gtrsim 100$  V/cm). For weak holding fields, it can describe well only the conductivity of warm and not very much heated electrons ( $T_e < 2$  K).

The numerical evaluations of  $v^{(a)}(T_e)$  and  $v^{(r)}(T_e)$  support the qualitative analysis of the momentum relaxation rate given at the end of preceding Section. Since the MW power used in our experiments is much lower than that providing the electron temperature saturation, we expect that the Boltzmann distribution of level occupancies is a reasonable approximation for evaluation of  $v^{(r)}(T_e)$ . For the conditions of the experiment of Ref. 7 ( $E_\perp = 3.15$  V/cm,  $T = 0.35$  K), the effective collision frequency calculated employing different models is shown

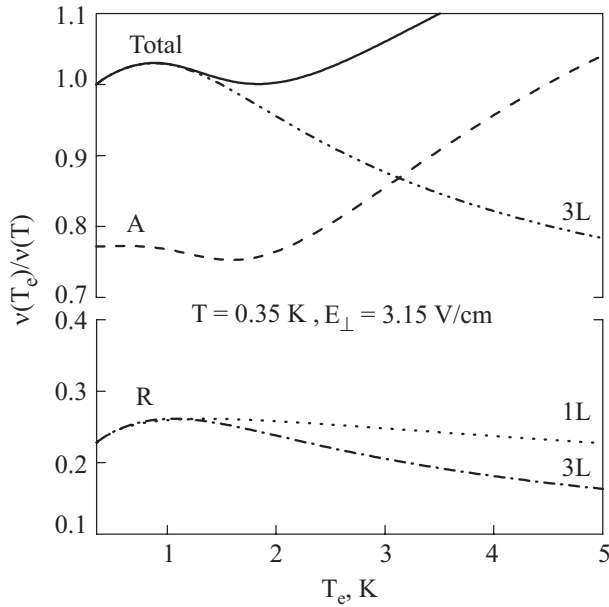


Fig. 5. Momentum collision frequency vs  $T_e$  normalized by  $v(T) \approx 1.52 \cdot 10^8 \text{ s}^{-1}$ : contribution from scattering by ripples (R) for 1-level (1L dotted line) and 3-level (3L dash-dotted line) models, contribution from vapor atoms (A) obtained in an all-level treatment, total  $v(T_e)$  for the 3-level model (dash-dot-dotted line) and for the all-level treatment of vapor-atom scattering as described in the text (solid line).

in Fig. 5. Though, at  $T_e = T$ , the electron-ripple collision rate is substantially lower than that induced by vapor atoms, it depends on electron temperature even at low MW powers, where  $v^{(a)}$  is approximately constant. Calculations conducted for the 1-level model result in a rapid increase in  $v^{(r)}$  with  $T_e$  (dotted line), which turns into a slow decrease at  $T_e > 1.3 \text{ K}$ .

Taking into account more surface levels affects mostly the decreasing part of the dependence  $v^{(r)}(T_e)$  which becomes sharper as shown by the dash-dotted line. The total collision frequency  $v = v^{(a)} + v^{(r)}$  of the 3-level model as a function of  $T_e$  preserves the conductivity maximum (dash-dot-dotted line) and decreases strongly at  $T_e > 1 \text{ K}$ . Even the inclusion of 400 levels in calculations of  $v^{(a)}$  (solid line) does not affect the maximum of the total collision frequency (here the contribution  $v^{(r)}(T_e)$  is still calculated for the 3-level model).

The above given theoretical results explain the mobility decrease at the photoresonance previously observed for low powers [7]. Even numerically, the change in the collision frequency at the maximum which is about 3% (Fig. 5) agrees well with typical changes of SE mobility observed in the experiment. Regarding the reversing of the sign of the effect observed at high powers, it agrees with the 3-level model considered here (dash-dot-dotted line), though this model cannot be applied for  $T_e > 1.2 \text{ K}$ . Therefore, this property should be verified by an all-level

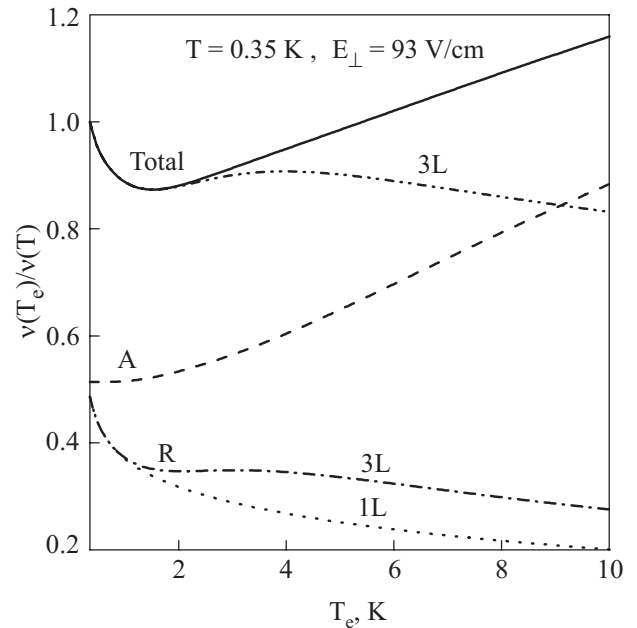


Fig. 6. Momentum collision frequency vs  $T_e$  calculated at  $E_{\perp} = 93 \text{ V/cm}$  and  $T = 0.35 \text{ K}$ : contribution from scattering by ripples (R) for 1-level (1L dotted line), and 3-level (3L dash-dotted line) models, contribution from vapor atoms (A) obtained in an all-level treatment, total  $v = v^{(a)} + v^{(r)}$  for the 3-level model (dash-dot-dotted line) and for the all-level treatment of vapor-atom scattering (solid line) as described in the text.

treatment which is very difficult for such a weak holding electric field. The existence of the collision frequency maximum at  $T_e \approx 0.88 \text{ K}$  leads to a complication of the shape of the conductivity resonance ( $\sigma(E_{\perp})$ ) induced by MW radiation of intermediate powers, which also agrees with observations [7].

In our experiments, the holding electric field is much stronger than that used in Ref. 7:  $E_{\perp} \approx 93 \text{ V/cm}$ . For such a field, at  $T_e = 0.48 \text{ K}$ , scattering by vapor atoms is dominant, and, as shown previously [10,18], the corresponding collision frequency of SEs increases steadily with heating. The experimental data relevant to this temperature and shown by the first data line of Fig. 2 are consistent with this conclusion. The photoresonance decreases the conductivity of SEs.

For the ambient temperature  $T = 0.35 \text{ K}$ , the dependence  $v(T_e)$  becomes completely different, as indicated in Fig. 6. At first, consider the contribution from the electron-ripple scattering only (lines R). For the models of the SE system analyzed here, the momentum collision frequency  $v^{(r)}$  mostly decreases with heating. The plateau feature which is seen for the 3-level model at  $T_2 \sim 2 \text{ K}$  remains remarkably even in models taking into account larger numbers of surface levels which we do not discuss in this publication. At the same time, the contribution from vapor atoms (line A) calculated for the all-level treatment increases steadily with  $T_e$ .



For the total collision frequency shown by the solid line, the contribution  $\nu^{(a)}$  was calculated using the all-level treatment, while  $\nu^{(r)}$  was taken from the 3-level analysis, as described above. Thus, instead of the maximum found above for  $E_{\perp} = 3.15$  V/cm, we have a minimum of the momentum relaxation rate. This minimum affects the shape of the conductivity resonance induced by the MW in the way which agrees with the corresponding data shown in Fig. 2. Even numerically, the decrease in  $\nu$  at the minimum is about 12% which is close to that obtained in our measurements. At high electron temperatures, we have a reversing of the sign of the effect which is opposite to that previously observed for the weak holding field: at low MW excitation powers, SE mobility increases with  $T_e$ , while at high powers it decreases.

At even lower  $T = 0.3$  K, the contribution from vapor atom scattering is substantial for high MW excitations as shown in Fig. 7. The total collision frequency normalized decreases stronger than at  $T = 0.35$  K, attains a minimum of about 0.76, and then very slowly increases reaching only 0.8 at  $T_e = 10$  K. In this case, we conclude that the shape of the conductivity resonance at medium powers should be similar to the Lorentzian shape, slightly affected at the maximum (the minimum of  $\nu$ ), as it is for the third data line in Fig. 2. According to the solid line of Fig. 7, vapor atoms restrict the total reduction in  $\nu$  and it should not exceed 24%. The observed reduction in  $\nu$  as shown in Fig. 2, is about 17% which is consistent with our calculations.

It should be noted that the absolute value of the momentum relaxation rate of SEs on liquid  $^3\text{He}$  previously measured employing different experimental setups [7,24]

used to differ from the theoretical value by a factor of 2. Our new data of  $\nu$  obtained by measuring  $\sigma_{xx}$  under a weak magnetic field providing the semi-classical transport regime are in much better agreement with the theory. For example, the out-of-resonance data shown in Fig. 2 give:  $\nu \simeq 15.3 \cdot 10^8 \text{ s}^{-1}$  ( $T = 0.48$  K),  $2.4 \cdot 10^8 \text{ s}^{-1}$  ( $T = 0.35$  K), and  $1.35 \cdot 10^8 \text{ s}^{-1}$  ( $T = 0.3$  K). The corresponding theoretical values for the total collision frequency are reasonably close:  $\nu \simeq 16 \cdot 10^8 \text{ s}^{-1}$  ( $T = 0.48$  K),  $2.6 \cdot 10^8 \text{ s}^{-1}$  ( $T = 0.35$  K), and  $1.46 \cdot 10^8 \text{ s}^{-1}$  ( $T = 0.3$  K). Thus, our new equilibrium conductivity data obtained for SEs on liquid  $^3\text{He}$  and the theory agree even numerically with the accuracy of about 7.5% in both the ripplon and vapor atom scattering regimes.

## 5. Conclusions

SEs on liquid helium exposed to resonance MW radiation represent an interesting system of hot electrons whose temperature can be much higher than the ambient temperature. The transport properties of such hot electrons along the interface can be described by the linear transport theory which allows to use them for probing the electron coupling with surface excitations of quantum liquids. At low ambient temperatures, the energy relaxation time of hot electrons is expected to be limited by emission of couples of short wavelength ripples ( $\hbar\omega_q \sim T_e/2$ ), which potentially could be used for experimental study of the spectrum of surface excitations of liquid  $^3\text{He}$  in a high energy range (up to about 5 K).

Our measurements of the conductivity resonance induced by MW radiation show that decay heating of SEs previously reported for scattering by vapor atoms remains to be an important factor in the ripplon scattering regime as well. It changes the momentum collision rate for electron scattering within the ground Rydberg level and leads to electron occupation of higher levels. At certain conditions, the interplay between scattering by ripples and scattering by vapor atoms affects strongly the shape of the conductivity resonance and leads to a reversing of the sign of the effect induced by MW radiation. Surprisingly, this reversing of the sign of the effect is opposite to that reported previously [7]. The theoretical analysis of SE relaxation rates in the presence of MW radiation given here indicates that conductivity changes induced by MW radiation are very sensitive to the magnitude of the MW frequency which determines the range of holding electric fields used for tuning to the resonance. This analysis explains well the conductivity variations observed, and eliminates the discrepancy between data obtained for different experimental setups.

## Acknowledgments

The work is partly supported by the Grant-in-Aids for Scientific Research from Monka-sho.

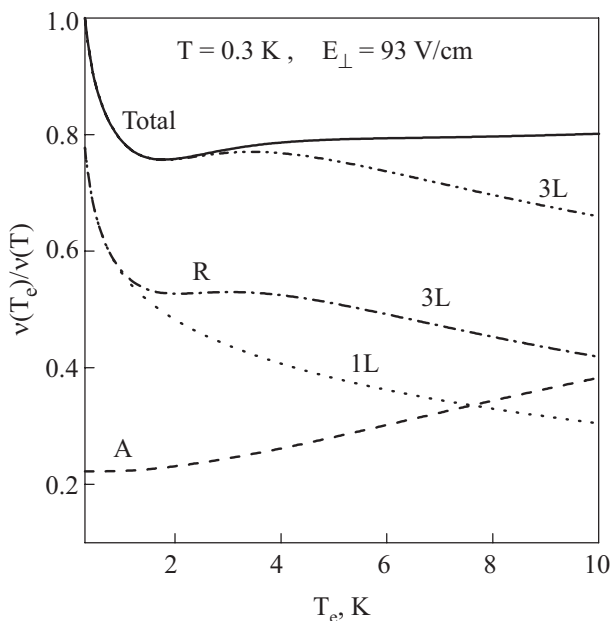


Fig. 7. Momentum collision frequency vs  $T_e$  calculated at  $E_{\perp} = 93$  V/cm and  $T = 0.3$  K. Notations are the same as in Fig. 6.

1. *Electrons on Helium and Other Cryogenic Substrates*, E.Y. Andrei (ed.), Kluwer Academic Pub., Dordrecht (1997).
2. Yu.P. Monarkha and K. Kono, *Two-Dimensional Coulomb Liquids and Solids*, Springer-Verlag, Berlin Heidelberg (2004).
3. C.C. Grimes and T.R. Brown, *Phys. Rev. Lett.* **32**, 280 (1974).
4. A.S. Rybalko, Yu.Z. Kovdrya, and B.N. Eselson, *Zh. Eksp. Teor. Phys.* **22**, 569 (1975) [*Sov. Phys.-JETP Lett.* **22**, 280 (1975)].
5. C.C. Grimes and G. Adams, *Phys. Rev. Lett.* **36**, 145 (1976).
6. V.S. Edel'man, *Zh. Eksp. Teor. Fiz.* **77**, 673 (1979) [*Sov. Phys. JETP* **50**, 338 (1979)].
7. A.P. Volodin and V.S. Edel'man, *Zh. Eksp. Teor. Fiz.* **81**, 368 (1981) [*Sov. Phys. JETP* **54**, 198 (1981)].
8. M.I. Dykman and L.S. Khazan *Zh. Eksp. Teor. Fiz.* **77**, 1488 (1979) [*Sov. Phys. JETP* **50**, 747 (1979)].
9. E. Teske, Yu.P. Monarkha, M. Seck, and P. Wyder, *Phys. Rev. Lett.* **82**, 2772 (1999).
10. D. Konstantinov, H. Isshiki, Yu.P. Monarkha, H. Akimoto, Keiya Shirahama, and K. Kono, *Phys. Rev. Lett.* **98**, 235302-1 (2007).
11. Yu. Monarkha, D. Konstantinov, and K. Kono, *Fiz. Nizk. Temp.* **33**, 942 (2007) [*Low Temp. Phys.* **33**, 718 (2007)].
12. E. Collin, W. Bailey, P. Fozooni, P.G. Frayne, P. Glasson, K. Harrabi, M.J. Lea, and G. Papageorgiou, *Phys. Rev. Lett.* **89**, 245301-1 (2002).
13. W.T. Sommer and D.J. Tanner, *Phys. Rev. Lett.* **27**, 1345 (1971).
14. M.J. Lea, A.O. Stone, P. Fozooni, and J. Frost, *J. Low Temp. Phys.* **85**, 67 (1991).
15. K. Shirahama and K. Kono, *J. Low Temp. Phys.* **104**, 237 (1996).
16. R. Loudon, *The Quantum Theory of Light*, Oxford Science, Oxford (2000).
17. T. Ando, *J. Phys. Soc. Jpn.* **44**, 765 (1978).
18. Yu. Monarkha, D. Konstantinov, and K. Kono, *J. Phys. Soc. Jpn.* **76**, 124702-1 (2007).
19. Yu.P. Monarkha, *Fiz. Nizk. Temp.* **4**, 1093 (1978) [*Sov. J. Low Temp. Phys.* **4**, 515 (1978)].
20. Yu.M. Vil'k, and Yu.P. Monarkha, *Fiz. Nizk. Temp.* **15**, 235 (1989) [*Sov. J. Low Temp. Phys.* **15**, 131 (1989)].
21. Yu.P. Monarkha and S.S. Sokolov, *Fiz. Nizk. Temp.* **32**, 1278 (2006) [*Low Temp. Phys.* **32**, 970 (2006)].
22. P.M. Platzman and G. Beni, *Phys. Rev. Lett.* **36**, 626 (1976).
23. M. Saitoh and T. Aoki, *J. Phys. Soc. Jpn.* **44**, 71 (1978).
24. K. Shirahama, S. Ito, H. Suto and K. Kono, *J. Low Temp. Phys.* **101**, 439 (1995).